

Expansion parallax of the planetary nebula IC 418

Lizette Guzmán¹, Laurent Loinard, Yolanda Gómez

*Centro de Radioastronomía y Astrofísica, Universidad Nacional Autónoma de México,
58089 Morelia, Michoacán, México*

and

Christophe Morisset

*Instituto de Astronomía, Universidad Nacional Autónoma de México,
04510 México, D.F., México*

ABSTRACT

In this paper, we present radio continuum observations of the planetary nebula IC 418 obtained at two epochs separated by more than 20 years. These data allow us to show that the angular expansion rate of the ionization front in IC 418 is 5.8 ± 1.5 mas yr⁻¹. If the expansion velocity of the ionization front is equal to the expansion velocity of the gas along the line of sight as measured by optical spectroscopy, then the distance to IC 418 must be 1.1 ± 0.3 kpc. Recent theoretical predictions appropriate for the case of IC 418, however, suggest that the ionization front may be expanding about 20% faster than the material. Under this assumption, the distance to IC 418 would increase to 1.3 ± 0.4 kpc.

Subject headings: planetary nebulae: general — planetary nebulae: individual (IC 418)
— astrometry — stars: late type

1. Introduction

The large uncertainties affecting distance estimates to planetary nebulae (PNe) continue to represent an important obstacle to our understanding of these objects. While the total number of PNe in the Milky Way has been estimated to be somewhere between 5,000 and 25,000 (Peimbert 1990, Zijlstra & Pottasch 1991, Acker et al. 1992), less than 50 have distances that have been measured individually with reasonable accuracy. About a third of these individual estimates are direct trigonometric parallax measurements (Harris et al. 2007), while the rest is based on a disparate set of indirect methods (e.g. spectroscopic parallax of the central star or of a resolved companion,

¹Also at: Jodrell Bank Centre for Astrophysics, University of Manchester, Manchester, M13 9PL, UK

cluster membership, reddening, or angular expansion). In addition, statistical methods, calibrated using PNe with individually measured distances, have been developed. A frequently used such statistical technique (called the Shklovsky method) is based on the assumption that the mass of ionized gas is the same for all PNe. This rather crude assumption has been refined by Daub (1982) and Cahn et al. (1992) who distinguish between density-bounded PNe (for which the Shklovsky constant mass hypothesis is assumed to hold) and radiation-bounded PNe (where the mass of ionized gas is taken to depend on the surface brightness of the nebula). For a recent review of various methods of distance determinations to PNe, see Phillips (2002).

A potentially reliable direct geometric method to estimate the distance of an individual PN is the so-called expansion parallax technique. In this method, the angular expansion of the source on the plane of the sky is measured, and compared to the expansion along the line of sight determined from optical spectroscopy. Traditionally, the angular expansion has been obtained from multi-epoch radio interferometric data gathered over a period of several years (Masson 1986), but measurements at optical wavelengths with the Hubble Space Telescope have also been used (Reed et al. 1999; Palen et al. 2002). This technique has been applied successfully to several PNe (Masson 1986, 1989; Gómez et al. 1993; Hajian et al. 1993, 1995; Kawamura & Masson 1996; Hajian & Terzian 1996; Christianto & Seaquist 1998; Guzman et al. 2006), and can provide distances accurate to about 20%. This is comparable to the accuracy obtained from existing trigonometric parallax measurements (Harris et al. 2007), and significantly better than the accuracy of statistical methods (e.g. Stanghellini et al. 2008). In this paper, we will apply the expansion parallax technique to the well studied PN IC 418.

The morphology of IC 418 (G215.2-24.2, PK 215-24.1, The Spirograph Nebula) is fairly simple: both at optical and radio wavelengths, it has an elliptical ring shape, with a major axis of $14''$ and a minor axis of $10''$. It is surrounded by a low-level ionized halo, which is itself enshrouded in a neutral envelope with an angular size of about $2'$ (Taylor & Pottasch 1987, Taylor et al. 1989). Widely discrepant estimates of the distance to IC 418 have been obtained using different statistical methods. To our knowledge, the shortest distance ever proposed is 360 pc (Acker 1978) whereas the largest one is 5.74 kpc (Phillips & Pottasch 1984). The Shklovsky method mentioned earlier gives a value of 1.9 kpc (Cahn & Kaler 1971). In recent years, the most popular value appears to have been 1 kpc (e.g. Meixner et al. 1996, Pottasch et al. 2004), although the reason for this is not entirely clear.

Table 1. List of observations.

Project	Epoch	Phase Calibrator	Bootstrapped Flux Density(Jy)	Restored Beam
AP116	1986 Jun 28 (1986.49)	0605-085	2.347 ± 0.008	$3''80 \times 3''08$; P.A.= 0°
AL716	2007 Nov 06 (2007.85)	0516-160	0.425 ± 0.005	$3''80 \times 3''08$; P.A.= 0°

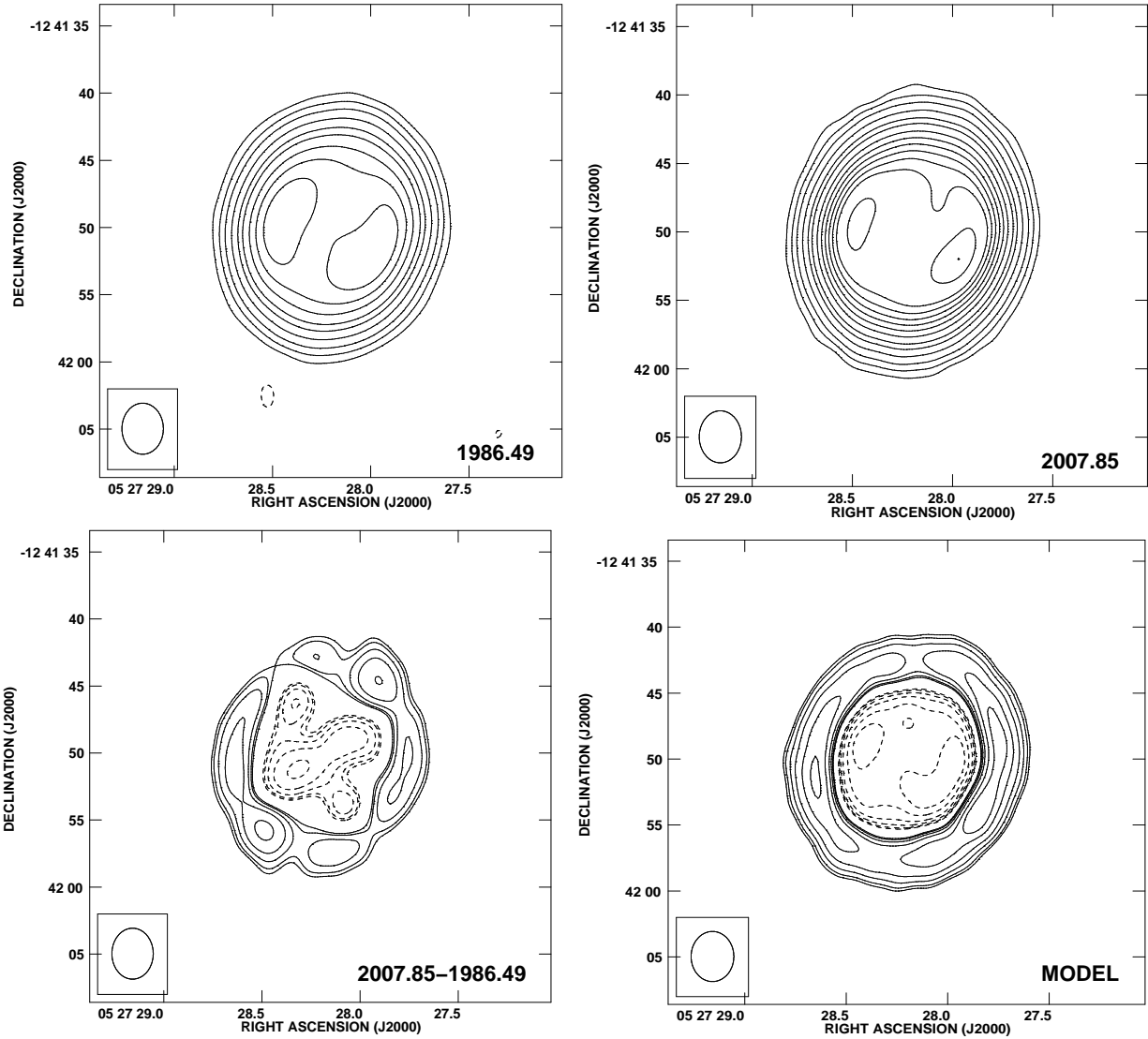


Fig. 1.— Top: contour images of the 6 cm continuum emission from IC 418 for 1986.49 (left) and 2007.85 (right). The contours are -5, 5, 10, 30, 50, 60, 80, 100, 150, 200, 250, 300 times $350 \mu\text{Jy}$, the average rms noise of the images. Bottom: contour images of the 6 cm difference image (left) and of the “model” (right) obtained as described in the text. The contours are -20, -15, -10, -7, -5, -4, 4, 5, 7, 10, 15, and 20 times $460 \mu\text{Jy}$, the rms noise of the difference image. The restoring beam ($3''.80 \times 3''.08$ with a position angle of 0°) is shown in the bottom left corner of each image.

2. Observations

The data (Tab. 1) were collected with the Very Large Array (VLA) of the NRAO¹ at 6 cm (5 GHz) in its second most extended (B) configuration on 1986, June 28 (1986.49) and 2007, November 06 (2007.85). This provides a time separation of 21.36 yr. The data were edited and calibrated using the Astronomical Image Processing System (AIPS) following standard procedures (see Table 1). The longest baselines were tapered down to increase the sensitivity, and self-calibration (in phase only) was applied. The resulting images are shown in Fig. 1.

3. Results and discussion

The difference image between the two epochs (new minus old) was produced following Guzman et al. (2006). It is shown in the bottom left panel of Fig. 1, and exhibits the typical concentric negative/positive pattern expected when expansion is present. It is possible to estimate the expansion rate of the nebula by comparing the difference image of the data with a model. That model can be built from the data of either epochs, but the best results are obtained using the dataset with the highest quality (corresponding to the second epoch in the present case). To generate the model difference, we image the data twice. The first imaging was made using a fixed pixel size of $0''.1$, whereas the second was made using pixels of $(1 + \epsilon) \times 0''.1$, with $\epsilon \geq 0$, but $\epsilon \ll 1$. We then formed the pixel-to-pixel subtraction between those two images. The physical size of the source, of course, does not depend on the chosen size of the pixel. But since the pixels are larger in the second case, the source occupies a smaller number of them. Therefore, the pixel-to-pixel subtraction is equivalent to subtracting from the real image of the source, a self-similarly shrunk (i.e. a de-magnified) version of itself. To identify the best model, we repeated the procedure described above for a set of values of ϵ . For each value, we compared the model difference with the real difference between the second and the first epoch. The best model clearly corresponds to the situation where the two differences are as similar to each other as possible. To obtain a quantitative measure of when that happens, we subtracted the two difference images, and calculated the r.m.s. of the resulting image. A plot of that r.m.s. as a function of ϵ (Fig. 2) shows that the minimum of the r.m.s. corresponds to a well-defined value of ϵ . That value was calculated using a fit to the data points with a quadratic form (blue curve in Fig. 3). This yields a value of $\epsilon = 0.018 \pm 0.005$.

The angular expansion rate can be determined from the value of ϵ using:

$$\dot{\theta} = \frac{\theta \epsilon}{\Delta t}.$$

The radius of maximum emission, θ , is estimated from the image at the second epoch to be $6''.700 \pm$

¹The National Radio Astronomy Observatory is operated by Associated Universities, Inc. under a cooperative agreement with the National Science Foundation.

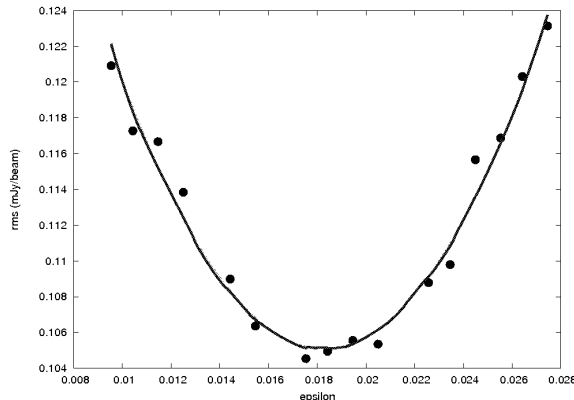


Fig. 2.— Residual r.m.s. value as a function of ϵ . The blue line shows the best quadratic fit.

$0''.006$, so $\dot{\theta} = 5.8 \pm 1.5 \text{ mas yr}^{-1}$. Since the radio emission considered here traces the ionized region of IC 418, $\dot{\theta}$ corresponds to the expansion rate of the ionization front.

To deduce the distance from the angular expansion rate calculated above, one must know the physical velocity v_{exp} at which the ionization front is expanding (e.g. Guzman et al. 2006):

$$\left[\frac{D}{pc} \right] = 211 \left[\frac{v_{exp}}{km \ s^{-1}} \right] \left[\frac{\dot{\theta}}{mas \ yr^{-1}} \right]^{-1}.$$

Traditionally, v_{exp} has been estimated using high spectral resolution observations of some emission lines and assuming a relation between the shape of the line profiles and the movement of the emitting gas. In the present case, we use the high resolution spectra of $H\beta$, [N II] and [O III] lines published by Gesicki et al. (1996). The $H\beta$ line is broad ($FWHM = 18 \text{ km s}^{-1}$, dominated by the thermal contribution), while the [O III] line is narrow and centered on the systemic velocity. The [N II] line, on the other hand, is double-peaked with each peak at $\pm 20 \text{ km s}^{-1}$ around the systemic velocity. Using a detailed 3D photoionization model of the nebula, Morisset and Georgiev (in prep.) reproduced these three profiles using a $V \propto R^4$ expansion law. According to this model, the expansion velocity near the outer edge of the nebula (where we detect expansion at radio wavelengths) is 30 km s^{-1} . This result is in good agreement with the radiation-hydrodynamic models of Schönberner et al. (2005) and Villaver et al. (2002). With this value of $v_{exp} = 30 \text{ km s}^{-1}$, we obtain a distance to IC 418 of $1.1 \pm 0.3 \text{ kpc}$.

There is a potential systematic effect discussed in detail by Mellema (2004) that ought to be taken into account. While the angular expansion measured using the VLA data corresponds to the progression of the ionization front (and is, therefore, a pattern velocity), the Doppler width deduced from spectral lines traces the expansion velocity of the material itself. For conditions appropriate for PNe, Mellema (2004) showed that the ionization front tends to expand somewhat faster than the material. Using their Fig. 5, we estimate that the expansion velocity of the ionization front in IC 418 is 1.2 ± 0.1 faster than the expansion velocity of the gas. Taking this effect into account

leads to a distance to IC 418 of 1.3 ± 0.4 kpc.

These two estimates of the distance are well within the broad range (0.36 to 5.74 kpc) of values obtained from statistical methods (see Sect. 1). They are also in very good agreement with the value of 1 kpc that has often been used recently, and with the value found by Morisset & Georgiev (in prep.): $d = 1.26 \pm 0.2$ kpc².

Two distance independent parameters can be derived from our observations. First, the dynamical age of the nebula can be calculated from the angular size and angular expansion rate: $\tau_{dyn} = \theta/\dot{\theta}$. We obtain $\tau_{dyn} \sim 1,200$ years. Second, the emission measure of the ionized region can be obtained from the observed parameters of the radio emission (we used the image at the second epoch, which is of better quality; the total 6 cm flux is 1.44 ± 0.01 Jy and the average deconvolved angular size of the emission is $13''.4 \pm 0''.01$). This yields an emission measure $EM = (5.05 \pm 0.01) \times 10^{-6} \text{ cm}^{-6} \text{ pc}$. Finally, the electron density and the mass of ionized gas can be calculated (also from the radio flux). We get $n_e = (6.2 \pm 1.7) (\frac{d}{1.1 \text{ kpc}})^{-0.5} \times 10^3 \text{ cm}^{-3}$, and $M_i = (8.7 \pm 2.4) (\frac{d}{1.1 \text{ kpc}})^{2.5} \times 10^{-2} M_{\odot}$. This is in reasonable agreement with the values found by Morisset & Georgiev (in prep.) from their detailed modeling ($n_e = 9 \times 10^3 \text{ cm}^{-3}$ and $M_i = 6 \times 10^{-2} M_{\odot}$).

4. Conclusions

In this paper, we presented observations of the 6 cm radio continuum emission from the well-studied planetary nebula IC 418 obtained at two epochs separated by more than 20 yr. These data allowed us to detect the angular expansion of the nebula, and to estimate its distance. Depending on the assumption made on the relative velocity of the matter and of the ionization front, we obtain a distance of 1.1 ± 0.3 kpc, or 1.3 ± 0.4 kpc.

LG, YG and LL acknowledge the support of DGAPA, UNAM and CONACYT (México). This research has made use of the SIMBAD database, operated at CDS, Strasbourg, France.

REFERENCES

- Acker, A. 1978, A&AS, 33, 367
- Acker, A., Cuisinier, F., Stenholm, B., & Terzan, A. 1992, A&A, 264, 217

² Morisset and Georgiev perform a detailed modeling of both the star and the nebula of IC418. They reproduce more than 140 nebular lines, as well as the HST images of the nebula, and the electron temperature and density diagnostics. All the main stellar emission and absorption lines are also reproduced. In this model, there is a degeneracy between the distance, the absolute magnitude, the size of the nebula, and the presence of clumps. They use evolutionary tracks to resolve the degeneracy and conclude that the filling factor is one. This leads to the distance of 1.26 ± 0.2 kpc mentioned here.

- Cahn, J. H. & Kaler, J. B. 1971, *ApJS*, 22, 319
- Cahn, J. H., Kaler, J. B., & Stanghellini, L. 1992, *A&AS*, 94, 399
- Christianto, H. & Seaquist, E. R. 1998, *AJ*, 115, 2466
- Daub, C.T., 1982, *ApJ*, 260, 612
- Gesicki, K., Acker, A., & Szczerba, R. 1996, *A&A*, 309, 907
- Gómez, Y., Rodríguez, L. F., & Moran, J. M. 1993, *ApJ*, 416, 620
- Guzmán, L., Gómez, Y., & Rodríguez, L. F. 2006, *Revista Mexicana de Astronomía y Astrofísica*, 42, 127
- Hajian, A. R. & Terzian, Y. 1996, *PASP*, 108, 258
- Hajian, A. R., Terzian, Y., & Bignell, C. 1993, *AJ*, 106, 1965
- Hajian, A. R., Terzian, Y. & Bignell, C. 1995, *AJ*, 109, 2600
- Harris, H. C., Dahn, C. C., Canzian, B., et al. 2007, *AJ*, 133, 631
- Kawamura, J. & Masson, C. 1996, *ApJ*, 461, 282
- Masson, C. R. 1986, *ApJ*, 302, L27
- Masson, C. R. 1989, *ApJ*, 336, 294
- Meixner, M., Skinner, C. J., Keto, E., Zijlstra, A., Hoare, M. G., Arens, J. F., & Jernigan, J. G. 1996, *A&A*, 313, 234
- Mellema, G. 2004, *A&A*, 416, 623
- Palen, S., Balick, B., Hajian, A. R., Terzian, Y., Bond, H. E. & Panagia, N. 2002, *AJ*, 123 2666
- Peimbert, M. 1990, *Revista Mexicana de Astronomía y Astrofísica*, 20, 119
- Phillips, J. P. 2002, *ApJS*, 139, 199
- Phillips, J. P., & Pottasch, S. R. 1984, *A&A* 130, 91
- Pottasch, S. R., Bernard-Salas, J., Beintema, D. A., & Feibelman, W. A. 2004, *A&A*, 423, 593
- Reed, D. S., Balick, B., Hajian, A. R., Klayton, T. L., Giovanardi, S., Casertano, S., Panagia, N., & Terzian, Y. 1999, *AJ*, 118, 2430
- Schönberner, D., Jacob, R., Steffen, M., Perinotto, M., Corradi, R. L. M., & Acker, A. 2005, *A&A*, 431, 963

Stanghellini, L., Shaw, R. A., & Villaver, E. 2008, *ApJ*, 689, 194

Taylor, A. R., Gussie, G. T., & Goss, W. M. 1989, *ApJ*, 340, 932

Taylor, A. R. & Pottasch, S. R. 1987, *A&A*, 176, L5

Villaver, E., Manchado, A., & García-Segura, G. 2002, *ApJ*, 581, 1204

Zijlstra, A. A. & Pottasch, S. R. 1991, *A&A*, 243, 478